

Supporting Information for : On the Evaluation of ^{95}Mo Nuclear Shielding and Chemical Shift of $[\text{Mo}_6\text{X}_{14}]^{2-}$ Clusters in Liquid Phase

Thi Thuong Nguyen,[†] Julie Jung,[†] Xavier Trivelli,[‡] Julien Trébosc,[¶] Stéphane
Cordier,[†] Yann Molard,[†] Laurent Le Pollès,[†] Chris J. Pickard,[§] Jérôme Cuny,^{*,||}
and Régis Gautier^{*,†}

*Institut des Sciences Chimiques de Rennes, UMR 6226 CNRS-Université de Rennes
1-Ecole Nationale Supérieure de Chimie de Rennes, 11 allée de Beaulieu, 35708 Rennes,
France, Unité de Glycobiologie Structurale et Fonctionnelle, UMR 8576 CNRS-Université
Lille 1 IFR 147, Cité Scientifique Bâtiment C9, 59655 Villeneuve d'Ascq, France, Unité
de Catalyse et Chimie du Solide, UMR 8181 CNRS-Université de Lille 1, 59655 Villeneuve
d'Ascq, France, Department of Physics and Astronomy, University College London, Gower
Street, London, WC1E6BT, UK, and Laboratoire de Chimie et Physique Quantiques
(LCPQ), Université de Toulouse III [UPS] and CNRS, 118 Route de Narbonne, F-31062
Toulouse, France*

E-mail: jerome.cuny@irsamc.ups-tlse.fr; regis.gautier@ensc-rennes.fr

Phone: +33 (0) 561556836. Fax: +33 (0) 561556065

Geometry optimisation of the isolated clusters

In this section, we present the geometry optimizations of $[\text{Mo}_6\text{Br}_{14}]^{2-}$ and $[\text{Mo}_6\text{I}_{14}]^{2-}$ using various sets of computational parameters: basis set, relativistic and solvent effects. In a purely octahedral symmetry, the geometry of each cluster is fully described by only three distances: Mo-Mo, Mo- X^a and Mo- X^i . These optimized distances for are presented on Fig. S1 and Fig. S2 for $[\text{Mo}_6\text{Br}_{14}]^{2-}$ and $[\text{Mo}_6\text{I}_{14}]^{2-}$, respectively.

Table S1: Optimized geometry of the $[\text{Mo}_6\text{Br}_{14}]^{2-}$ cluster obtained using various set of computational parameters. All the calculations have been performed using the PBE exchange-correlation functional. Implicit solvent (water) calculations are indicated between parentheses. The averaged experimental values are obtained from an X-ray analysis of the $\text{Cu}_2\text{Mo}_6\text{Cl}_{14}$ solid-state compound.¹

Basis Set	Relativistic Treatment	Mo-Mo (Å)	Mo-Br ⁱ (Å)	Mo-Br ^a (Å)
TZP	NR	2.675 (2.668)	2.700 (2.685)	2.686 (2.735)
	RS	2.686 (2.678)	2.674 (2.666)	2.665 (2.697)
	SO	2.686 (2.678)	2.675 (2.666)	2.666 (2.697)
TZ2P	NR	2.616 (2.605)	2.701 (2.679)	2.702 (2.775)
	RS	2.647 (2.638)	2.645 (2.639)	2.644 (2.666)
	SO	2.647 (2.638)	2.645 (2.639)	2.644 (2.666)
QZ4P	NR	2.666 (2.658)	2.634 (2.630)	2.634 (2.650)
	RS	2.649 (2.642)	2.629 (2.625)	2.626 (2.642)
	SO	2.649 (2.642)	2.629 (2.626)	2.626 (2.641)
Experimental¹		2.629	2.590	2.610

*To whom correspondence should be addressed

[†]Institut des Sciences Chimiques de Rennes, UMR 6226 CNRS-Université de Rennes 1-Ecole Nationale Supérieure de Chimie de Rennes, 11 allée de Beaulieu, 35708 Rennes, France

[‡]Unité de Glycobiologie Structurale et Fonctionnelle, UMR 8576 CNRS-Université Lille 1 IFR 147, Cité Scientifique Bâtiment C9, 59655 Villeneuve d'Ascq, France

[¶]Unité de Catalyse et Chimie du Solide, UMR 8181 CNRS-Université de Lille 1, 59655 Villeneuve d'Ascq, France

[§]Department of Physics and Astronomy, University College London, Gower Street, London, WC1E6BT, UK

^{||}Université de Toulouse III (UPS)

Table S2: Optimized geometry of the $[\text{Mo}_6\text{I}_{14}]^{2-}$ cluster obtained using various set of computational parameters. All the calculations have been performed using the PBE exchange-correlation functional. Implicit solvent (water) calculations are indicated between parentheses. The averaged experimental values are obtained from an X-ray analysis of the $\text{Cu}_2\text{Mo}_6\text{Cl}_{14}$ solid-state compound.¹

Basis Set	Relativistic Treatment	Mo-Mo (Å)	Mo-I ⁱ (Å)	Mo-I ^a (Å)
TZP	NR	2.701 (2.697)	2.853 (2.843)	2.932 (2.979)
	RS	2.711 (2.704)	2.847 (2.842)	2.921 (2.957)
	SO	2.710 (2.704)	2.851 (2.845)	2.922 (2.958)
TZ2P	NR	2.618 (2.613)	2.877 (2.856)	2.948 (3.030)
	RS	2.678 (2.671)	2.813 (2.811)	2.900 (2.928)
	SO	2.678 (2.671)	2.815 (2.813)	2.902 (2.929)
QZ4P	NR	2.722 (2.713)	2.808 (2.805)	2.894 (2.920)
	RS	2.695 (2.685)	2.803 (2.802)	2.884 (2.908)
	SO	2.694 (2.685)	2.806 (2.805)	2.885 (2.909)
Experimental¹		2.672	2.770	2.860

Discussion on the nature of the density functional

The present study was carried out using the PBE exchange-correlation functional only, although this parameter has also been shown to play an important part in the calculation of ^{95}Mo nuclear shielding parameters.^{2,3} However, as stated by Bühl in its study of molybdenum complexes,² the widely used B3LYP hybrid functional performs considerably worse than some GGA functionals for molybdenum in contrast to other transition metals. Consequently, an exhaustive study on the influence of the exchange-correlation functional on the ^{95}Mo δ_{iso} of the $[\text{Mo}_6\text{X}_{14}]^{2-}$ clusters would be required. Thus, although such a study was not the main focus of the present contribution, to roughly assess the extent of this influence we carried out B3LYP calculations for the 150 $[\text{MoO}_4(\text{H}_2\text{O})_{10}]^{2-}$ molecular clusters discussed in the main text. The mean and the standard deviations of the ^{95}Mo σ_{iso} are equal to -759 ppm and 158 ppm, respectively, which is significantly different from the results presented on Figure 9 of the main manuscript. These significant differences show how important is the treatment of the exchange-correlation interaction in such calculations and the need of an exhaustive study of this question.

Self-Diffusion Coefficient of the Water Molecules

In order to investigate the liquid-like character of our molecular dynamics simulations, we calculated the self-diffusion coefficient of the water molecules D_{self} . Fig. S1 displays the mean-square displacement (MSD) curves for the first set of simulations at 310 K, 340 K, 370 K, 400 K and 450 K. Each curve was obtained by averaging the MSD of each independent water molecule oxygen atom in the corresponding simulation. D_{self} was then calculated from the slope of a linear fit of these curves in the range 6-10 ps following the Einstein's relation:

$$D_{\text{self}} = \frac{1}{6} \lim_{t \rightarrow \infty} \frac{d}{dt} \langle |\mathbf{r}_i(t) - \mathbf{r}_i(0)|^2 \rangle \quad (1)$$

The values of D_{self} are reported in Tab. S3. These values are consistent with the results of Sit and Marzari who studied in details the structural and dynamical properties of liquid heavy water simulated using the PBE functional in the range 325-400 K.⁴ In this work, the authors demonstrated that at least 10 ps of equilibration times are necessary to further calculate meaningful thermodynamic properties. It is worth pointing that all our simulations were properly equilibrated during 10 ps before our production runs. Furthermore, the authors also demonstrated that below 375 K the simulation lead to a frozen-like state of the water whereas at 400 K, a liquid-like state is reached. The results reported in Tab. S3 and Fig. S1 also show a frozen-like character at 310, 340 and 370 K and a liquid-like character at 400 and 450 K.

Consequently, the simulations we performed at 400 K are clearly the most representative of an ambient temperature solution of MoO_4^{2-} . We thus choose to consider the corresponding average ^{95}Mo isotropic nuclear shielding value (see Tab. 4 of the main text) as the best approximation to the correct ambient temperature value. To test if a more diffusive liquid water would lead to an improved sampling of the system, and to a different average ^{95}Mo σ_{iso} value for MoO_4^{2-} , we preformed simulations at 450 K. Although this temperature is experimentally beyond the boiling point of heavy water, the high freezing temperature of

PBE heavy water suggests that the simulations at 450 K still correctly represent liquid heavy water and not a boiling state of the phase diagram. As can see on Tab. 4 of the main text, the average ^{95}Mo isotropic nuclear shielding of MoO_4^{2-} at 450 K (-899 ppm) is closed to the value obtained at 400 K (-896 ppm) which shows that a good convergence is obtained at this temperature. Interestingly, the values obtained at 340 K (-893 ppm) and 370 K (-895 ppm) are also very closed to the 400 K value although the simulations show a frozen-like behaviour. Only the value at 310 K is significantly different from the others which certainly comes from a wrong sampling of the system due to its strong frozen-like character.

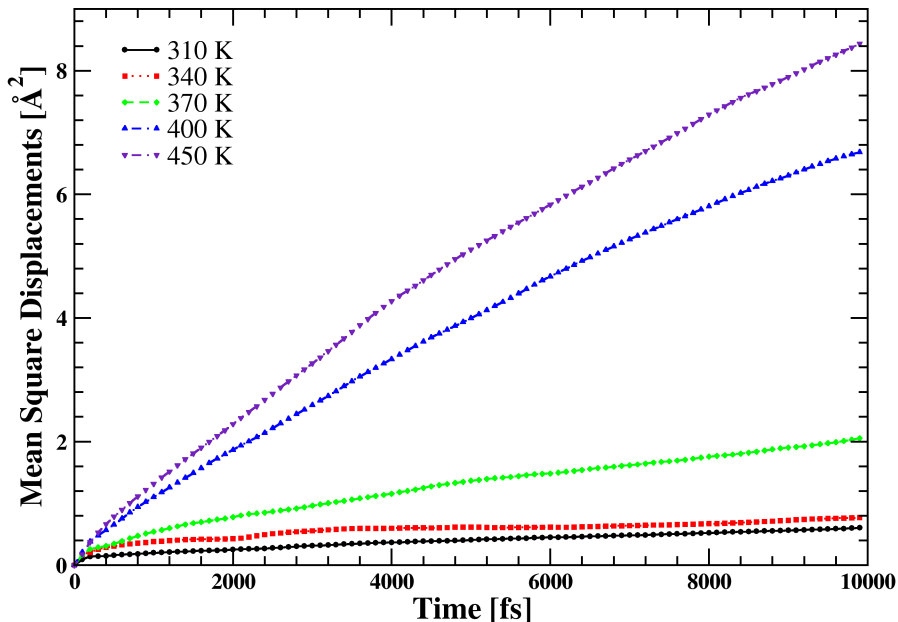


Figure S1: Mean-square displacement of the water molecules calculated from the production runs of the first set of simulations at 310 K (black plain line, circles), 340 K (red dotted line, square), 370 K (green dashed line, diamond), 400 K (blue dashed dotted line, triangle up) and 450 K (indigo dashed double dotted line, triangle down).

Table S3: Self-diffusion coefficient of the water molecules calculated from the first set of molecular dynamics simulations.

Temperature	310 K	340 K	370 K	400 K	450 K	Exp.
$D_{\text{self}} (10^{-5}\text{cm}^2.\text{s}^{-1})$	0.20	0.23	0.77	2.50	3.26	1.87^5

References

- (1) Peppenhorst, A.; Keller, H.-L. *Z. Anorg. Allg. Chem.* **1996**, *622*, 663–669.
- (2) Bühl, M. *Chem.–Eur. J.* **1999**, *5*, 3514–3522.
- (3) Cuny, J.; Sykina, K.; Fontaine, B.; Le Polles, L.; Pickard, C. J.; Gautier, R. *Phys. Chem. Chem. Phys.* **2011**, *13*, 19471–19479.
- (4) Sit, P. H.-L.; Marzari, N. *J. Chem. phys.* **2005**, *122*, 204510.
- (5) Mills, R. *J. Phys. Chem.* **1973**, *77*, 685–688.